

A novel arrangement of silicate tetrahedra in the uranyl silicate sheet of oursinite, (Co_{0.8}Mg_{0.2})[(UO₂)(SiO₃OH)]₂(H₂O)₆

KARRIE-ANN KUBATKO AND PETER C. BURNS*

Department of Civil Engineering and Geological Sciences, University of Notre Dame, 156 Fitzpatrick Hall, Notre Dame, Indiana 46556, U.S.A.

ABSTRACT

Oursinite is a rare Co-bearing uranyl silicate of the uranophane group. The structure of oursinite, (Co_{0.8}Mg_{0.2})[(UO₂)(SiO₃OH)]₂(H₂O)₆, is orthorhombic, space group *Cmca*, $a = 7.0494(5)$, $b = 17.550(1)$, $c = 12.734(1)$ Å, $V = 1575.4(2)$ Å³, $Z = 4$. It was solved by direct methods and refined on the basis of F^2 for all unique reflections using least-squares techniques to an agreement index ($R1$) of 2.66%. The structure contains an approximately linear (UO₂)²⁺ uranyl ion that is present as a uranyl pentagonal bipyramid, one symmetrically distinct SiO₃OH acid silicate group, and one M²⁺(OH,H₂O)₆ octahedron (M is dominated by Co). The uranyl pentagonal bipyramids and silicate tetrahedra are linked by the sharing of edges and vertices, giving a sheet based upon the uranophane anion topology. Adjacent sheets are linked by M²⁺(OH,H₂O)₆ octahedra located in the interlayer, and by hydrogen bonds. Each M²⁺(OH,H₂O)₆ octahedron contains two OH groups that are apical ligands of silicate tetrahedra in adjacent uranyl silicate sheets. Although several uranophane-group minerals contain sheets that are based upon the uranophane anion topology, the oursinite sheet involves novel orientations of silicate tetrahedra.

Keywords: Oursinite, uranyl silicate, uranium, crystal structure

INTRODUCTION

Uranyl silicates of the uranophane group are probably the most abundant of the uranyl minerals, and are common in the oxidized portions of U deposits (Finch and Ewing 1992). The crystal structures of most uranophane-group minerals have been reported: uranophane, Ca[(UO₂)(SiO₃OH)]₂(H₂O)₅ (Ginderow 1988); β-uranophane, Ca[(UO₂)(SiO₃OH)]₂(H₂O)₅ (Viswanathan and Harneit 1986); boltwoodite, (K_{0.56}Na_{0.42})[(UO₂)(SiO₃OH)](H₂O)_{1.5} (Burns 1998); sklodowskite, Mg[(UO₂)(SiO₃OH)]₂(H₂O)₆ (Ryan and Rosenzweig 1977); cuprosklodowskite, Cu[(UO₂)(SiO₃OH)]₂(H₂O)₆ (Rosenzweig and Ryan 1975); kasolite, Pb[(UO₂)(SiO₄)](H₂O) (Rosenzweig and Ryan 1977). All are composed of sheets of uranyl pentagonal bipyramids and silicate tetrahedra, with lower-valence cations and H₂O groups located in the interlayers of the structures.

Uranophane-group minerals are important for understanding the genesis of U deposits, as well as water-rock interactions within such deposits. They occur as alteration products of UO₂ and spent nuclear fuel under conditions similar to those expected in the proposed nuclear waste repository at Yucca Mountain, Nevada (Wronkiewicz et al. 1992, 1996; Finch et al. 1999; Finn et al. 1996). Burns et al. (2004) provided evidence that uranophane can incorporate Np⁵⁺, which may significantly impact the mobility of Np⁵⁺ in a geological repository.

Oursinite, with formula Co[(UO₂)(SiO₃OH)]₂(H₂O)₆, was described from Shinkolobwe, Democratic Republic of Congo, by Deliens and Piret (1983). Although it was immediately recognized as a member of the uranophane group, details of its crystal structure remain unknown. Here we provide the details of the structure of oursinite, with comparison to other minerals of the uranophane group.

EXPERIMENTAL METHODS

Specimen locality

Oursinite occurs as translucent white to pale yellow acicular prisms and needles ranging up to 1 mm in maximum dimension. Although crystals are rare, the mineral closely resembles other uranophane-group minerals, such as sklodowskite. Crystals used in the current study are from specimen RC3934 from l'Institut Royal des Sciences Naturelles in Brussels, Belgium. The specimen is from the Shinkolobwe mine in Democratic Republic of Congo, and contains mostly lepersonnite-(Gd) as well as becquerelite, curite, uranophane, sklodowskite, and oursinite.

Chemical analysis

The single crystal used for the collection of X-ray data was mounted in epoxy, polished, and coated with carbon. Four analyses were done using a Cameca SX-50 electron microprobe with a focused beam at 15 kV and 20 nA. The crystal was analyzed for Co, Mg, Na, Al, Si, K, Ca, Mn, Fe, Zn, and U, but only Co, Mg, Si, and U were detected. Standards were as follows: synthetic diopside-composition glass (Mg, Si), UO₂ (U), and synthetic CoO (Co). The analyses confirmed that Co is the dominant constituent in the interlayer cation sites, and the Co:Mg ratios derived from the four analyses ranged from 74:26 to 81:19, in accord with the refined site occupancies of the structure model, which gave a Co:Mg ratio of 80:20.

Collection of X-ray data

A crystal of oursinite with dimensions 10 × 10 × 80 μm was attached to a tapered glass fiber and mounted on a Bruker 3-circle diffractometer equipped with an APEX 4 K CCD detector and graphite monochromated MoK α radiation. A sphere of data was collected to 69° 2 θ with a crystal-to-detector distance of 4.67 cm, frame widths of 0.3° in ω , and 180 s spent counting per frame. Crystallographic parameters are provided in Table 1. Data were reduced and corrected for Lorentz, polarization, and background effects using the Bruker program SAINT. A semi-empirical correction for absorption was applied by modeling the crystal as an ellipsoid, which reduced R_{int} (1853 reflections) from 3.39 to 2.61%. A total of 15 359 reflections was collected, of which 1748 were unique, and 1374 were classed as observed ($|F_o| \geq 4\sigma_f$).

* E-mail: pburns@nd.edu

Structure solution and refinement

The Bruker SHELXTL Version 5 system of programs was used for the solution and refinement of the structure of oursinite. Scattering curves for neutral atoms, together with anomalous-dispersion corrections, were taken from International Tables for Crystallography, vol. IV (Ibers and Hamilton 1974). Analysis of the data indicated space group *Cmca*, consistent with the earlier findings of Deliens and Piret (1983), who suggested space groups *Aba2* or *Abam*. The structure was solved in space group *Cmca* by direct methods, and was refined on the basis of F^2 for all unique reflections. Occupancy refinement for the M^{2+} site was done using atomic scattering factors of Co and Mg, with the total occupancy of the site constrained to unity; the site occupancy refined to 80.0(1)% Co and 20.0(1)% Mg. H atoms were located in difference-Fourier maps calculated following refinement of the positions of the heavier atoms, and were refined with the soft constrain that O-H distances equal -0.96 \AA . The final agreement index ($R1$) was 2.66%, which was calculated for the 1374 unique observed reflections ($|F_o| > 4\sigma_f$). Additional details of the structure refinement are provided in Table 1. The final structure model included refined atomic coordinates, anisotropic displacement parameters for the non-H atoms, and a weighting scheme of the structure factors. Final atomic coordinates and anisotropic displacement parameters are listed in Table 2. Interatomic distances and selected bond angles are given in Table 3. Observed and calculated structure-factors are given in Table 4¹.

RESULTS

Cation polyhedra

The crystal structure of oursinite contains a single symmetrically unique U^{6+} cation that is strongly bonded to two O atoms, forming an approximately linear $(UO_2)^{2+}$ uranyl ion (Ur). The uranyl ion is coordinated by five O atoms located at the equatorial vertices of a pentagonal bipyramid that is capped by the O_{Ur} atoms. The $\langle U-O_{Ur} \rangle$ and $\langle U-O_{eq} \rangle$ ($eq = \text{equatorial}$) bond lengths are 1.805 and 2.355 \AA , both of which are within the range expected for such bonds in well-refined structures (Burns et al. 1997).

The structure contains a single symmetrically distinct Si^{4+} cation that is tetrahedrally coordinated by three O atoms and one

OH group, resulting in an acid silicate group. The $\langle Si-O \rangle$ bond length is 1.632 \AA , and the longest bond, with length 1.668(5) \AA , extends to the OH group.

The single symmetrically distinct M^{2+} cation site in oursinite contains Co and Mg, and is coordinated by two OH and four H_2O groups arranged at the vertices of a distorted octahedron with a $\langle M^{2+}-OH, H_2O \rangle$ bond length of 2.088 \AA .

Polyhedral connectivity

Consistent with all other uranyl silicates of the uranophane group, the structure of oursinite contains sheets of uranyl pentagonal bipyramids and silicate tetrahedra that share edges and vertices (Fig. 1a). The sheets contain chains of edge-sharing uranyl pentagonal bipyramids, with silicate tetrahedra attached to both sides of the chain by sharing equatorial edges of the uranyl polyhedra. Linkages between adjacent chains of uranyl and silicate polyhedra is by the sharing of vertices of silicate tetrahedra with uranyl polyhedra of adjacent chains.

The $M^{2+}(OH, H_2O)_6$ octahedra are located in the interlayer of the structure, between adjacent uranyl silicate sheets (Fig. 2). The octahedra include two OH groups that are apical ligands of

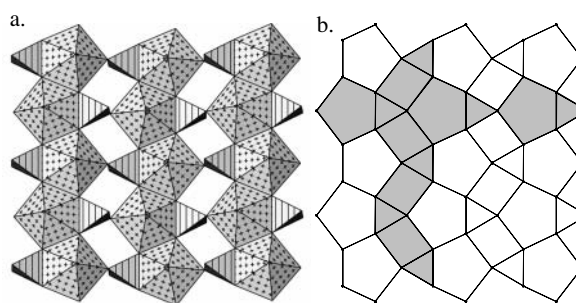


FIGURE 1. Polyhedral representation of the uranyl silicate sheet in the structure of oursinite (a) and its corresponding sheet anion topology (b). Uranyl polyhedra are shaded with crosses, and silicate tetrahedra with parallel lines.

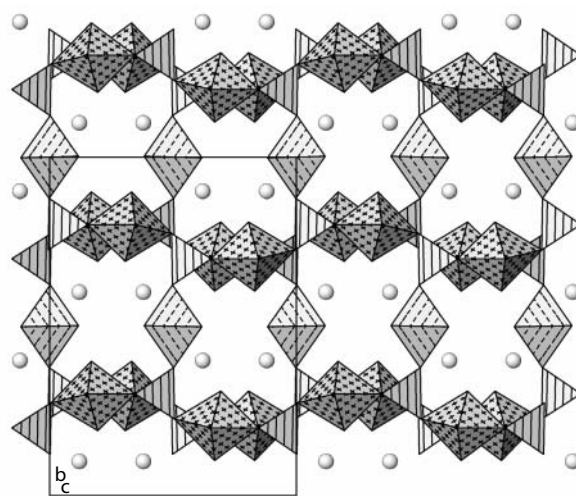


FIGURE 2. Polyhedral representation of the crystal structure of oursinite projected onto (100). Uranyl polyhedra are shaded with crosses, silicate tetrahedra with parallel lines, and $M^{2+}(OH, H_2O)_6$ octahedra are shaded with broken parallel lines.

TABLE 1. Crystallographic data and details of the structure refinement of oursinite

Formula	$(Co_{0.8}Mg_{0.2})[(UO_2)(SiO_3OH)]_2(H_2O)_6$
Space group	<i>Cmca</i>
<i>a</i> (\AA)	7.0494(5)
<i>b</i> (\AA)	17.550(1)
<i>c</i> (\AA)	12.734(1)
<i>V</i>	1575.4(2)
<i>Z</i>	4
$\rho_{\text{calculated}}$ (g/cm^3)	3.766
μ (mm^{-1})	21.79
<i>F</i> (000)	1588
Crystal size (μm)	$10 \times 10 \times 80$
Radiation	MoK α
Reflections collected	15359
Independent reflections	1748
Unique $ F_o \geq 4\sigma_f$	1374
Refinement method	Full-matrix least-squares on F^2
<i>R1</i> (%)	2.66
<i>wR2</i> (%)	5.18
<i>S</i>	0.88
Largest diff peak ($e/\text{\AA}^3$)	3.33/-1.30

¹Deposit item AM-05-004, Table 4. Deposit items are available two ways: For a paper copy contact the Business Office of the Mineralogical Society of America (see inside front cover of recent issue) for price information. For an electronic copy visit the MSA web site at <http://www.minsocam.org>, go to the American Mineralogist Contents, find the table of contents for the specific volume/issue wanted, and then click on the deposit link there.

TABLE 2. Atomic coordinates and equivalent displacement parameters for oursinite

	Occ.	x	y	z	U_{eq}	U_{11}	U_{22}	U_{33}	U_{23}	U_{13}	U_{12}
U	100%	0	0.20567(1)	0.18049(2)	0.01210(6)	0.00754(8)	0.01777(1)	0.01106(9)	0.0007(1)	0	0
Si	100%	0	0.2991(1)	-0.0716(1)	0.0140(3)	0.0131(7)	0.0198(9)	0.0091(6)	0.0017(6)	0	0
Co	80(1)%	0	0.5	0	0.0218(4)	0.0242(8)	0.0186(8)	0.0225(8)	-0.0014(5)	0	0
Mg	20(1)%	0	0.5	0	0.0218(4)	0.0242(8)	0.0186(8)	0.0225(8)	-0.0014(5)	0	0
O1	100%	0	0.1035(2)	0.1685(4)	0.023(1)	0.020(2)	0.015(2)	0.034(3)	-0.001(2)	0	0
O2	100%	0	0.3082(3)	0.1944(3)	0.022(1)	0.030(3)	0.023(3)	0.014(2)	-0.002(2)	0	0
O3	100%	0	0.2261(3)	0.0060(3)	0.0177(9)	0.019(2)	0.022(2)	0.012(2)	-0.001(2)	0	0
O4	100%	0.1756(4)	0.3003(2)	-0.1538(2)	0.0188(6)	0.009(1)	0.035(2)	0.013(1)	0.003(1)	0.001(1)	-0.001(1)
OH5	100%	0	0.3779(2)	0.0016(3)	0.022(1)	0.034(3)	0.017(2)	0.017(2)	-0.003(2)	0	0
OW6	100%	0.2006(7)	0.4979(3)	0.1177(4)	0.050(1)	0.052(3)	0.036(3)	0.062(3)	-0.013(2)	-0.029(2)	0.001(2)
OW7	100%	0.5	0.3998(3)	0.1212(4)	0.036(1)	0.050(4)	0.026(3)	0.031(3)	0.002(2)	0	0
H1	100%	0	0.382(5)	0.076(2)	0.05						
H2	100%	0.275(7)	0.483(4)	0.062(3)	0.05						
H3	100%	0.231(9)	0.549(2)	0.136(5)	0.05						
H4	100%	0.5	0.369(4)	0.183(4)	0.05						
H5	100%	0.5	0.377(5)	0.053(3)	0.05						

silicate tetrahedra of both adjacent sheets, as well as four H₂O groups that are also located in the interlayer.

Hydrogen bonding

The probable network of hydrogen bonding, as derived from constrained least-squares refinement of the H atom positions against the X-ray data, is illustrated in Figure 3. The O5 position, which corresponds to an OH group of the silicate tetrahedron, donates a hydrogen bond that is accepted by the O2 position (O_{Ur}). As such, this hydrogen bond bridges silicate and uranyl polyhedra within the same sheet. The O6 position, which is an H₂O group that is bonded to the M²⁺ cation, donates hydrogen bonds that are accepted by O1, an O_{Ur} atom of a uranyl polyhedron in an adjacent sheet, and by O7 of the H₂O group that is held in the structure by hydrogen bonding only. In addition to accepting the hydrogen bond from H2, the O7 position donates two hydrogen bonds that extend to the O3 position, an equatorial ligand of a uranyl pentagonal bipyramid, and O2 (O_{Ur}). Both hydrogen bonds from any given O7 position are accepted by anions located in the same uranyl silicate sheet.

Related structures

The uranophane anion topology (Fig. 1b) contains pentagons, squares, and triangles, and is the basis for various sheets that occur in uranyl minerals and synthetic compounds (Burns et al. 1996; Locock and Burns 2003). In the case of the uranophane-group minerals, the sheet is obtained from the anion topology by populating all pentagons with uranyl ions, giving uranyl pentagonal bipyramids, and each of the triangles in the topology correspond to a face of a silicate tetrahedron. With the exception of kasolite, an acid silicate group occurs in each of these uranyl silicate sheets.

Despite being based upon an identical sheet anion topology, not all uranyl silicate sheets in uranophane-group minerals are identical. Consider the anion topology given in Figure 1b, in which two distinct and mutually perpendicular chain types are identified by shading: those composed of edge sharing squares and triangles (designated ST, vertical in Fig. 1b), and those composed of pentagons and triangles that share edges and vertices (designated PT, horizontal in Fig. 1b). Uranyl silicate sheets in uranophane-group minerals are distinguished by the orientations of silicate tetrahedra along these chains. In the case of the sheets found in uranophane, boltwoodite, kasolite, cuprosklodowskite,

TABLE 3. Bond lengths (Å) and angles (°) for oursinite

U1-O1	1.800(4)	Si1-O3	1.618(5)
U1-O2	1.809(4)	Si1-O4, e	1.622(3) × 2
U1-O3	2.251(4)	Si1-OH5	1.668(5)
U1-O4a, b	2.314(3) × 2	<Si-O>	1.632
U1-O4c, d	2.449(3) × 2		
O1-U1-O2	179.2(2)	M-OW6,e,f,g	2.061(4) × 4
<U1-O _{Ur} >	1.805	M-OH5, f	2.142(5) × 2
<U1-O _{eq} >	2.355	<M-O>	2.088

Notes: a = -x + 1/2, -y + 1/2, -z; b = x - 1/2, -y + 1/2, -z; c = -x, -y + 1/2, z + 1/2; d = x, -y + 1/2, z + 1/2; e = -x, y, z; f = -x, -y + 1, -z; g = x, -y + 1, -z.

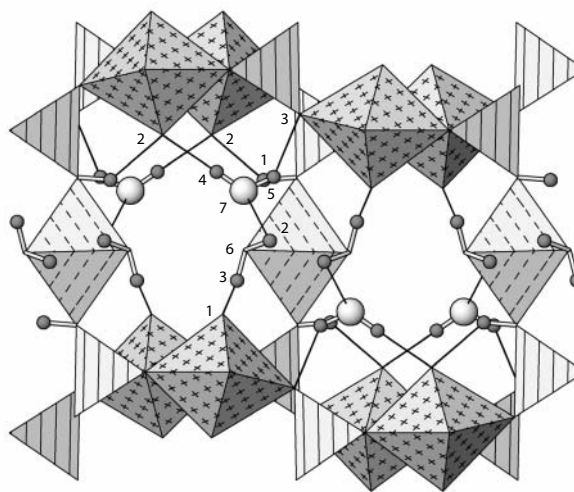


FIGURE 3. The hydrogen bonding network in the structure of oursinite. Legend as in Figure 2. H-acceptor bonds are shown as solid lines. Atom labels correspond to numbers in Table 2.

and sklodowskite (Fig. 4a), the apical ligands of the silicate tetrahedra along the ST chain point alternately up (U) and down (D), with the sequence UDUDUD... In the same sheet, the tetrahedra contained within a single PT chain either point all up or all down. In the case of the sheet found in β -uranophane (Fig. 4b), silicate tetrahedra along the ST chain alternate as UUD-DUDD..., whereas those along the PT chains either all point down or up. The oursinite sheet is novel among uranyl silicates in its orientation of the silicate tetrahedra (Fig. 4c). Along both the ST chains and the PT chains the tetrahedra alternate UPUPUP..., thus it is distinct from both the uranophane and β -uranophane populations of the uranophane anion topology in the orientation

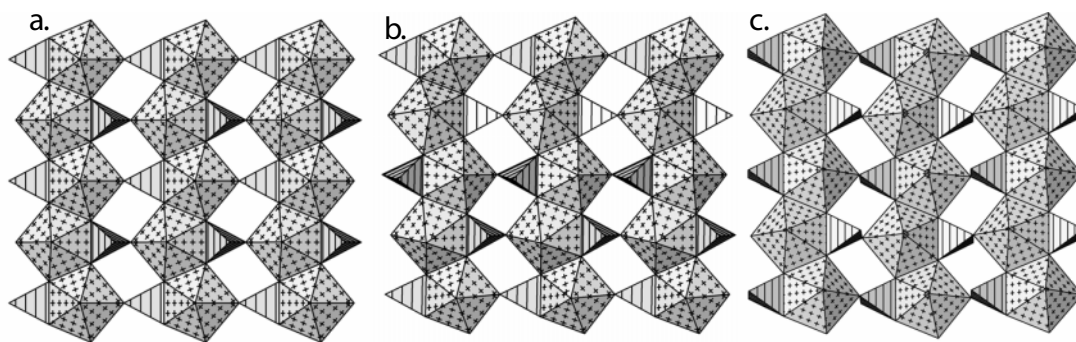


FIGURE 4. Uranyl silicate sheets from uranophane-group minerals: (a) uranophane, boltwoodite, cuprosklodowskite, sklodowskite, and kasolite; (b) β -uranophane; (c) oursinite.

of tetrahedra along the PT chains. Identical geometrical isomers are known in the cases of uranyl vanadates, phosphates, and arsenates (Locock and Burns 2003).

The structure of sklodowskite is closely related to that of oursinite; it contains almost identical cation polyhedra, although Mg dominates in the octahedral site rather than Co. The fundamental difference between these structures is the orientation of the silicate tetrahedra within the sheets, which requires different alignment of the sheets. Given the similar sizes of Mg^{2+} and Co^{2+} , it seems reasonable to predict a complete Mg-Co solid solution series in both sklodowskite and oursinite; should this be the case, the two structures would constitute polymorphs, as with the structures of uranophane and β -uranophane.

ACKNOWLEDGMENTS

Michel Deliens provided the crystal of oursinite used in this study. Ian Steele, University of Chicago, provided the microprobe analyses. This research was funded by the Environmental Management Sciences Program of the Office of Science, U.S. Department of Energy, grant DE-FG07-97ER14820.

REFERENCES CITED

- Breese, N. and O'Keeffe, M. (1991) Bond valence parameters for solids. *Acta Crystallographica*, B47, 192–197.
- Burns, P.C. (1998) The structure of boltwoodite and implications of solid-solution towards sodium boltwoodite. *Canadian Mineralogist*, 36, 1069–1075.
- Burns, P.C., Miller, M.L., and Ewing, R.C. (1996) U^{6+} minerals and inorganic phases: a comparison and hierarchy of crystal structures. *Canadian Mineralogist*, 34, 845–880.
- Burns, P.C., Ewing, R.C., and Hawthorne, F.C. (1997) The crystal chemistry of hexavalent uranium: polyhedral geometries, bond-valence parameters, and polymerization of polyhedra. *Canadian Mineralogist*, 35, 1551–1570.
- Burns, P.C., Deely, K.M., and Skanthakumar, S. (2004) Neptunium incorporation into uranyl compounds that form as alteration products of spent nuclear fuel: Implications for geologic repository performance. *Radiochimica Acta*, 92, 151–159.
- Deliens, M. and Piret, P. (1983) L'oursinite ($\text{Co}_{0.86}\text{Mg}_{0.10}\text{Ni}_{0.04}$) $0.2\text{UO}_2 \cdot 2\text{SiO}_2 \cdot 6\text{H}_2\text{O}$, nouveau mineral de Shinkolobwe, Shaba, Zaïre. *Bulletin of Mineralogy*, 196, 305–308.
- Finch, R. and Ewing, R. (1992) The corrosion of uraninite under oxidizing conditions. *Journal of Nuclear Materials*, 190, 133–156.
- Finch, R., Buck E., Finn, P., and Bates, J. (1999) Oxidative corrosion of spent UO_2 fuel in vapor and dripping groundwater at 90 °C. *Material Research Society Symposium Proceedings*, 556, 431–438.
- Finn, P.A., Hoh, J.C., Wolf, S.F., Slater, S.F., and Bates, J.K. (1996) The release of uranium, plutonium, cesium, strontium, technetium and iodine from spent fuel under unsaturated conditions. *Radiochimica Acta*, 74, 65–71.
- Ginderow, D. (1988) Structure de l'uranophane alpha, $\text{Ca}(\text{UO}_2)_2(\text{SiO}_3\text{OH})2.5\text{H}_2\text{O}$. *Acta Crystallographica*, C44, 421–424.
- Ibers, J.A. and Hamilton, W.C., Eds. (1974) *International Tables for X-ray Crystallography*, IV. The Kynoch Press, Birmingham, U.K.
- Locock, A.J. and Burns, P.C. (2003) Structures and syntheses of framework triuranil diarsenate hydrates. *Journal of Solid State Chemistry*, 176, 18–26.
- Rosenzweig, A. and Ryan, R.R. (1975) Refinement of the crystal structure of cuprosklodowskite, $\text{Cu}[(\text{UO}_2)_2(\text{SiO}_3\text{OH})_2] \cdot 6\text{H}_2\text{O}$. *American Mineralogist*, 60, 448–453.
- óóó (1977) Kasolite, $\text{Pb}(\text{UO}_2)(\text{SiO}_3) \cdot \text{H}_2\text{O}$. *Crystal Structure Communications*, 6, 617–621.
- Ryan, R.R. and Rosenzweig, A. (1977) Sklodowskite, $\text{MgO} \cdot 2\text{UO}_3 \cdot 2\text{SiO}_2 \cdot 7\text{H}_2\text{O}$. *Crystal Structure Communications*, 6, 611–615.
- Viswanathan, K. and Harneit, O. (1986) Refined crystal structure of β -uranophane $\text{Ca}(\text{UO}_2)_2(\text{SiO}_3\text{OH})2.5\text{H}_2\text{O}$. *American Mineralogist*, 71, 1489–1493.
- Wronkiewicz, D., Bates, J., Gerding, T., Veleckis, E., and Tani, B. (1992) Uranium release and secondary phase formation during unsaturated testing of UO_2 at 90 °C. *Journal of Nuclear Materials*, 190, 107–127.
- Wronkiewicz, D., Bates, J., Wolf, S., and Buck, E. (1996) Ten year results from unsaturated drip tests with UO_2 at 90 °C: implications for the corrosion of spent nuclear fuel. *Journal of Nuclear Materials*, 1238, 178–95.

MANUSCRIPT ACCEPTED JULY 9, 2005

MANUSCRIPT RECEIVED JANUARY 28, 2004

MANUSCRIPT HANDLED BY MARIA FRANCA BRIGATTI